Supplementary Material: Unsupervised Domain Adaptation for Tubular Structure Segmentation Across Different Anatomical Sources

Yuxiang An
yuan5699@uni.sydney.edu.au

Dongnan Liu
dongnan.liu@sydney.edu.au

Weidong Cai
tom.cai@sydney.edu.au

School of Computer Science
The University of Sydney
Sydney, Australia

1 Data Preprocessing

We used four datasets in this paper to validate the effectiveness of our approach, ISBI [2], VNC [8], DRIVE [14], and CHASE [6]. Electron microscope images (ISBI and VNC) are grayscale images and fundus images (DRIVE and CHASE) are RGB three-channel color images. Therefore we grayscaled the fundus images. Since the regions of interest of electron microscope images and fundus images are different, the region of interest of electron microscope images is the set of all pixels, and the region of interest of fundus images is the set of pixels inside the eyeball. To prevent incomplete global information and reduce discrepancies caused by patching, we rescaled all images to 512×512 using cubic interpolation. Simultaneously, labels were resized to the corresponding 512×512 size using nearest neighbor interpolation. Our enhanced images are obtained by summing the feature maps obtained by Jerman [10] and Frangi [5] after black and white conversion with the original image.

1.1 Comparison Experiments

We validate the effectiveness of our approach with a comprehensive comparison of nine unsupervised domain adaptation methods on four datasets. These nine methods are DANN [7], UMDA-SNA [11], DCDA [12], SAM-UDA [4], ADANet [16], FFO [15], SFUDA [1], MIC [9], and LA-UDA [3]. Figure 1 demonstrates the complete comparison results. Table 1 quantifies the metrics differences between the different UDA methods, showing that the segmentation results of our method are more accurate. Our method is able to obtain more continuous and more complete segmentation results in fundus images, which is more obvious at the ends of blood vessels. Our approach yields segmentation outcomes with reduced noise in electron microscopy images. Furthermore, it achieves more precise segmentation
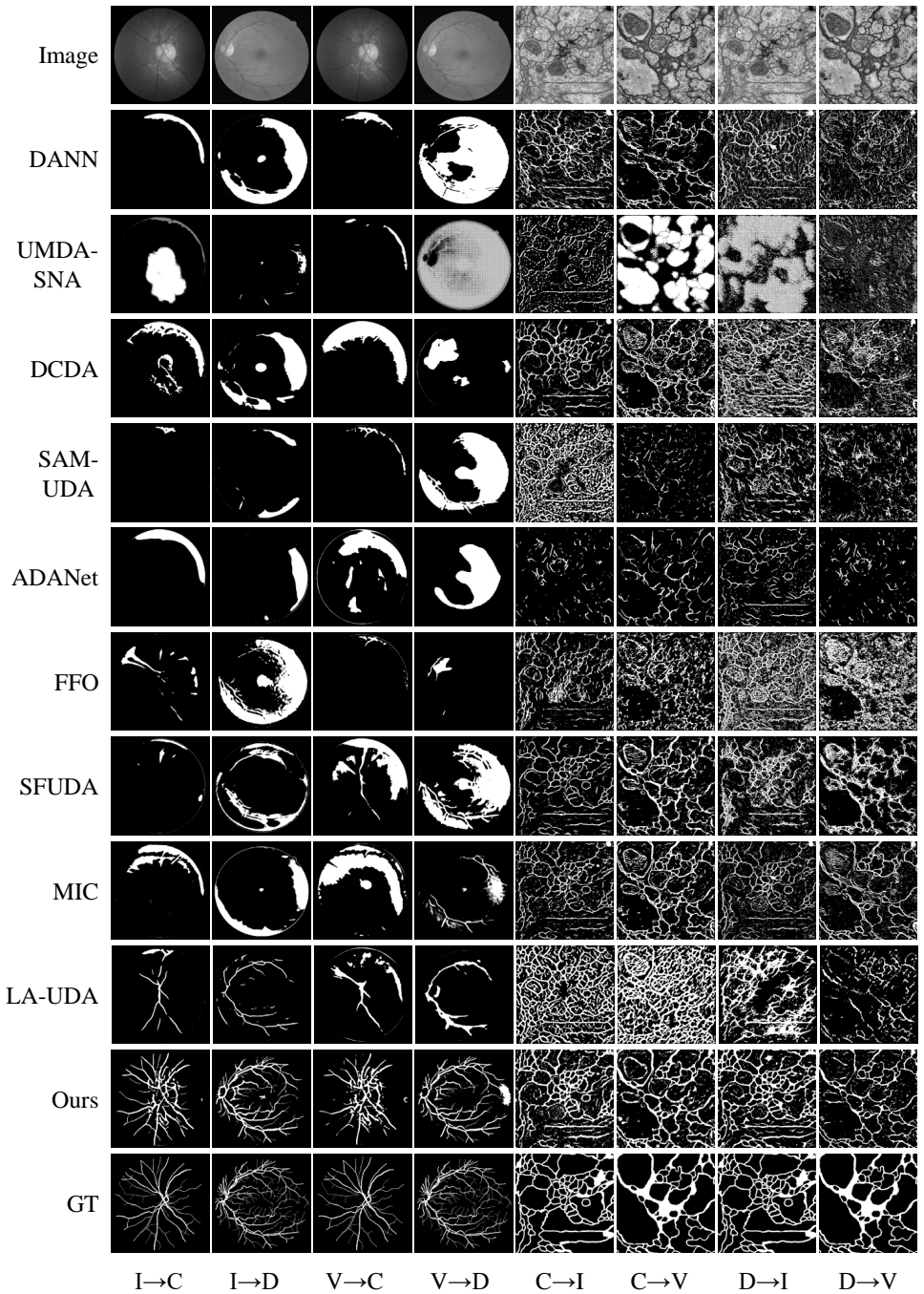
Figure 1: Visualization examples of comparative experiments. I: ISBI, V: VNC, C: CHASE, D: DRIVE.
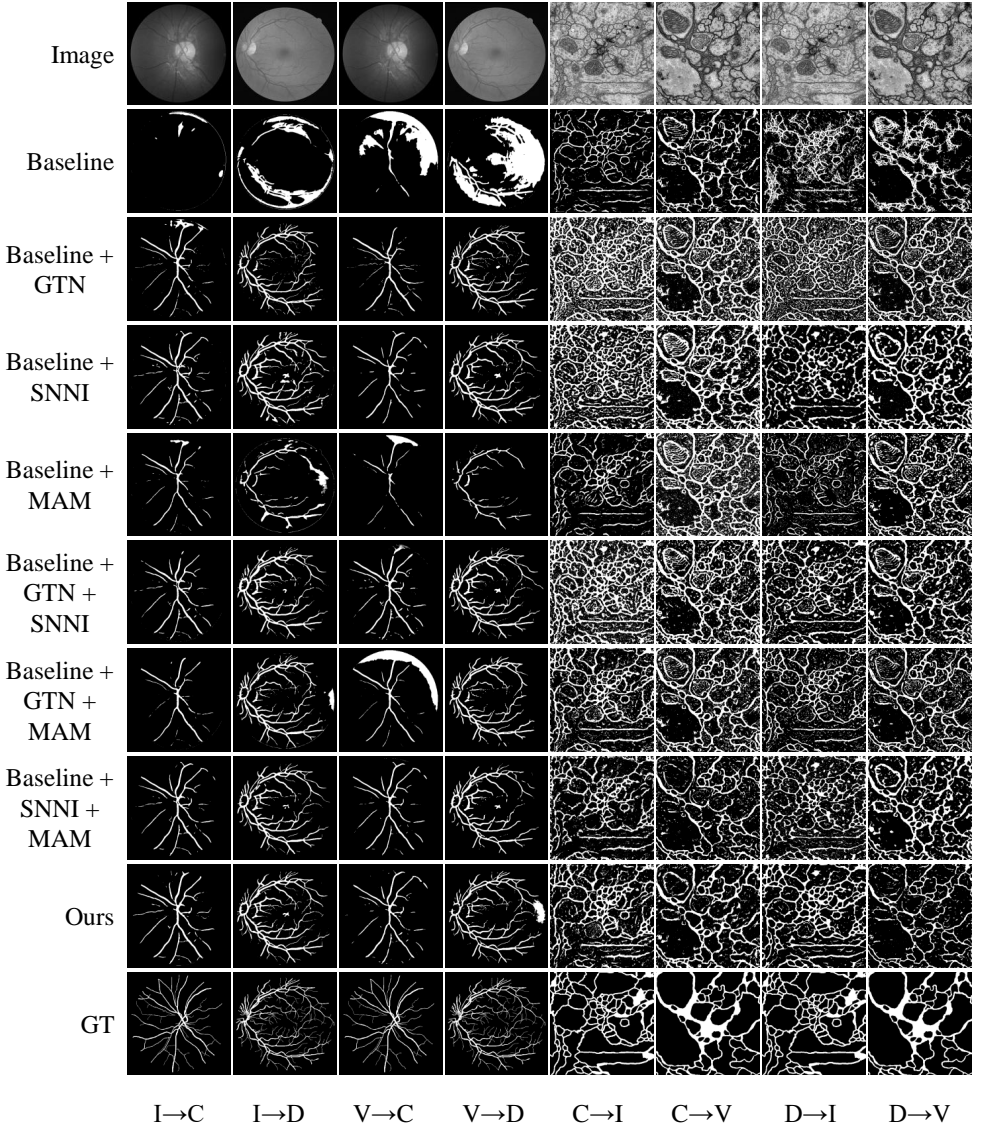
Figure 2: Visualization examples of ablation studies. I: ISBI, V: VNC, C: CHASE, D: DRIVE.

results for the thicker regions of the tubular structure. The results of the comparison experiments demonstrate that UDA methods proposed for a single anatomical source do not work well in a multi-anatomical source setting. We believe that this is due to the variability in the data characteristics of the tubular structures of different anatomical sources and the great variability in the background noise of different anatomical sources. In addition, the fact that these methods do not provide explicit feature constraints for the segmentation targets is also a reason for their failure.

Table 1: Comparison experiments. I: ISBI, V: VNC, C: CHASE, D: DRIVE.

Method	I→C	I→D	V→C	V→D	C→I	C→V	D→I	D→V
U-Net(No adaptation) [■]	7.79%	2.88%	16.56%	22.84%	36.13%	20.13%	36.79%	27.76%
U-Net(Supervised) [■]	80.59%	80.87%	80.59%	80.87%	78.73%	88.30%	78.73%	88.30%
DANN [■]	12.34%	13.75%	13.43%	19.27%	57.88%	62.81%	47.88%	44.84%
UMDA-SNA [■]	15.87%	10.85%	13.75%	21.35%	42.36%	32.24%	37.70%	19.57%
DCDA [■]	15.92%	14.17%	16.33%	20.16%	61.23%	63.06%	46.59%	45.28%
SAM-UDA [■]	14.10%	10.78%	13.92%	16.89%	43.43%	39.95%	40.35%	22.83%
ADANet [■]	11.43%	9.69%	14.31%	12.49%	65.40%	36.48%	41.69%	23.56%
FFO [■]	19.73%	18.13%	14.80%	20.04%	48.57%	36.67%	46.90%	35.33%
SFUDA [■]	13.79%	26.40%	14.80%	26.43%	54.44%	64.75%	54.15%	59.51%
MIC [■]	15.42%	10.86%	14.85%	15.13%	61.85%	68.74%	59.14%	64.57%
LA-UDA [■]	36.76%	39.70%	24.67%	26.34%	56.19%	44.15%	45.29%	47.80%
Ours	**60.46%**	**67.11%**	**53.93%**	**61.68%**	**67.52%**	**70.84%**	**68.05%**	**69.94%**

Table 2: Ablation studies. I: ISBI, V: VNC, C: CHASE, D: DRIVE.

Method	I-C	I-D	V-C	V-D	C-I	C-V	D-I	D-V
Baseline	13.79%	26.40%	14.80%	26.43%	54.44%	64.75%	54.15%	59.51%
Baseline+GTN	51.92%	60.62%	36.47%	59.00%	53.26%	57.48%	56.42%	58.82%
Baseline+SNNI	56.60%	63.23%	50.79%	60.96%	54.79%	63.06%	62.36%	64.99%
Baseline+MAM	55.06%	34.30%	43.36%	36.24%	65.89%	57.01%	60.02%	62.03%
Baseline+GTN+SNNI	55.98%	64.38%	52.10%	61.29%	55.42%	60.95%	61.22%	65.73%
Baseline+GTN+MAM	34.28%	57.25%	27.67%	57.48%	64.29%	63.60%	64.47%	62.53%
Baseline+SNNI+MAM	59.35%	64.48%	53.32%	59.24%	64.54%	66.66%	63.04%	65.92%
Ours	**60.46%**	**67.11%**	**53.93%**	**61.68%**	**67.52%**	**70.84%**	**68.05%**	**69.94%**

1.2   Ablation Studies

We verify the effectiveness of the three proposed modules in the framework through ablation studies. We use the segmentation network in [■] as a baseline and attach the proposed modules to the framework separately. The ablation results show that all three of our proposed modules improve the segmentation accuracy. Figure 2 shows visualization results of ablation studies. Table 2 lists the quantitative results of the ablation studies. Through ablation studies, we also found that in some cases, the performance of using GTN and MAM is not as good as using either of the two modules alone. We believe that the use of GTN + MAM drives the model to refine the segmentation of the source domain without enhancing the segmentation network, thus decreasing the segmentation performance of the target domain. The effectiveness of the two combinations, GTN + SNNI and SNNI + MAM, proves our theory.

References

[1] Yuxiang An, Dongnan Liu, and Weidong Cai. Unsupervised domain adaptation for neuron membrane segmentation based on structural features. In *IEEE International Conference on Multimedia and Expo*, pages 948–953, 2023.

[2] Albert Cardona, Stephan Saalfeld, Stephan Preibisch, Benjamin Schmid, Anchi Cheng, Jim Pulokas, Pavel Tomancak, and Volker Hartenstein. An integrated micro-and

macroarchitectural analysis of the drosophila brain by computer-assisted serial section electron microscopy. *PLoS Biology*, 8(10):e1000502, 2010.

[3] Julio Ivan Davila Carrazco, Pietro Morerio, Alessio Del Bue, and Vittorio Murino. Learnable data augmentation for one-shot unsupervised domain adaptation. In *British Machine Vision Conference*, 2023.

[4] Inseop Chung, Jayeon Yoo, and Nojun Kwak. Exploiting inter-pixel correlations in unsupervised domain adaptation for semantic segmentation. In *Proceedings of the IEEE/CVF Winter Conference on Applications of Computer Vision*, pages 12–21, 2023.

[5] Alejandro F Frangi, Wiro J Niessen, Koen L Vincken, and Max A Viergever. Multiscale vessel enhancement filtering. In *International Conference on Medical Image Computing and Computer-Assisted Intervention*, pages 130–137, 1998.

[6] Muhammad Moazam Fraz, Paolo Remagnino, Andreas Hoppe, Bunyarit Uyyanonvara, Alicja R Rudnicka, Christopher G Owen, and Sarah A Barman. An ensemble classification-based approach applied to retinal blood vessel segmentation. *IEEE Transactions on Biomedical Engineering*, 59(9):2538–2548, 2012.

[7] Yaroslav Ganin, Evgeniya Ustinova, Hana Ajakan, Pascal Germain, Hugo Larochelle, François Laviolette, Mario March, and Victor Lempitsky. Domain-adversarial training of neural networks. *Journal of Machine Learning Research*, 17(59):1–35, 2016.

[8] Stephan Gerhard, Jan Funke, Julien Martel, Albert Cardona, and Richard Fetter. Segmented anisotropic sstem dataset of neural tissue. *Figshare*, 2013.

[9] Lukas Hoyer, Dengxin Dai, Haoran Wang, and Luc Van Gool. Mic: Masked image consistency for context-enhanced domain adaptation. In *Proceedings of the IEEE/CVF Conference on Computer Vision and Pattern Recognition*, pages 11721–11732, 2023.

[10] Tim Jerman, Franjo Pernuš, Boštjan Likar, and Žiga Špiclin. Enhancement of vascular structures in 3d and 2d angiographic images. *IEEE Transactions on Medical Imaging*, 35(9):2107–2118, 2016.

[11] Jinping Liu, Hui Liu, Subo Gong, Zhaohui Tang, Yongfang Xie, Huazhan Yin, and Jean Paul Niyoyita. Automated cardiac segmentation of cross-modal medical images using unsupervised multi-domain adaptation and spatial neural attention structure. *Medical Image Analysis*, 72:102135, 2021.

[12] Linkai Peng, Li Lin, Pujin Cheng, Ziqi Huang, and Xiaoying Tang. Unsupervised domain adaptation for cross-modality retinal vessel segmentation via disentangling representation style transfer and collaborative consistency learning. In *IEEE International Symposium on Biomedical Imaging*, pages 1–5, 2022.

[13] Olaf Ronneberger, Philipp Fischer, and Thomas Brox. U-net: Convolutional networks for biomedical image segmentation. In *International Conference on Medical Image Computing and Computer-Assisted Intervention*, pages 234–241, 2015.

[14] Joes Staal, Michael D Abràmoff, Meindert Niemeijer, Max A Viergever, and Bram Van Ginneken. Ridge-based vessel segmentation in color images of the retina. *IEEE Transactions on Medical Imaging*, 23(4):501–509, 2004.

[15] Shengsheng Wang, Zihao Fu, Bilin Wang, and Yulong Hu. Fusing feature and output space for unsupervised domain adaptation on medical image segmentation. *International Journal of Imaging Systems and Technology*, 33(5):1672–1681, 2023.

[16] Ting Zhang, Zihang Gao, Zhaoying Liu, Syed Fawad Hussain, Muhammad Waqas, Zahid Halim, and Yujian Li. Infrared ship target segmentation based on adversarial domain adaptation. *Knowledge-Based Systems*, 265:110344, 2023.